Nicotinic acid– and monomethyl fumarate–induced flushing involves GPR109A expressed by keratinocytes and COX-2–dependent prostanoid formation in mice

Julien Hanson,[1,2,3] Andreas Gille,[2] Sabrina Zwykiel,[2] Martina Lukasova,[1,2] Björn E. Clausen,[4] Kashan Ahmed,[1,2] Sorin Tunaru,[1,2] Angela Wirth,[1,2] and Stefan Offermanns[1,2,5]

[1]Department of Pharmacology, Max-Planck-Institute for Heart and Lung Research, Bad Nauheim, Germany. [2]Institute of Pharmacology, University of Heidelberg, Heidelberg, Germany. [3]Department of Medicinal Chemistry, CIRM, University of Liège, Liège, Belgium. [4]Department of Immunology, Erasmus Medical Center, Rotterdam, The Netherlands. [5]Medical Faculty, Goethe University Frankfurt, Frankfurt, Germany.

The antidyslipidemic drug nicotinic acid and the antipsoriatic drug monomethyl fumarate induce cutaneous flushing through activation of G protein–coupled receptor 109A (GPR109A). Flushing is a troublesome side effect of nicotinic acid, but may be a direct reflection of the wanted effects of monomethyl fumarate. Here we analyzed the mechanisms underlying GPR109A-mediated flushing and show that both Langerhans cells and keratinocytes express GPR109A in mice. Using cell ablation approaches and transgenic cell type–specific GPR109A expression in *Gpr109a*$^{-/-}$ mice, we have provided evidence that the early phase of flushing depends on GPR109A expressed on Langerhans cells, whereas the late phase is mediated by GPR109A expressed on keratinocytes. Interestingly, the first phase of flushing was blocked by a selective cyclooxygenase-1 (COX-1) inhibitor, and the late phase was sensitive to a selective COX-2 inhibitor. Both monomethyl fumarate and nicotinic acid induced PGE_2 formation in isolated keratinocytes through activation of GPR109A and COX-2. Thus, the early and late phases of the GPR109A-mediated cutaneous flushing reaction involve different epidermal cell types and prostanoid-forming enzymes. These data will help to guide new efficient approaches to mitigate nicotinic acid–induced flushing and may help to exploit the potential antipsoriatic effects of GPR109A agonists in the skin.

Introduction

Nicotinic acid (also referred to as niacin) has been used for decades to treat dyslipidemic conditions, and it was the first lipid-modifying drug for which a beneficial effect on cardiovascular mortality was reported (1–4). There has recently been a renewed interest in the pharmacological effects of nicotinic acid, since it is by far the most efficacious drug to increase HDL-cholesterol plasma levels (5, 6). Unfortunately, the beneficial effects of nicotinic acid are accompanied by unwanted effects, of which cutaneous vasodilation (i.e., flushing) is the most problematic (7, 8). Nicotinic acid–induced flushing lasts for about 1–2 hours and is associated with a sensation of tingling and burning, causing many patients to discontinue nicotinic acid therapy. The nicotinic acid–induced flush phenomenon was first observed shortly after the discovery of nicotinic acid as a vitamin that can be used to treat pellagra (9, 10). In both humans and animal models, nicotinic acid–induced flushing has been reported to be biphasic, with the first peak in intensity occurring shortly after the beginning of the reaction and the second peak after the first has faded (11, 12).

The fact that nicotinic acid–induced flushing can be reduced by coadministration of cyclooxygenase inhibitors (13–15) indicates that prostanoids are important mediators of nicotinic acid–dependent flushing. A role for prostanoids in the flushing reaction is also indicated by the fact that plasma levels of vasodilatory prostanoids like prostaglandin D_2 (PGD_2) and PGE_2 and their metabolites increase after nicotinic acid treatment (13–17). More recently, genetic and pharmacological approaches provided evidence that PGD_2 and PGE_2 mediate the flushing reaction (12, 18, 19), and a PGD_2 DP_1 receptor antagonist was recently approved in Europe for the prevention of nicotinic acid–induced flushing (20, 21).

Nicotinic acid–induced flushing is initiated by activation of G protein–coupled receptor 109A (GPR109A), as mice lacking this receptor no longer respond to nicotinic acid with flushing (12). GPR109A is expressed in various immune cells of the skin; in particular, epidermal Langerhans cells have been shown to express GPR109A and to be involved in the flushing reaction (22, 23). Interestingly, the antipsoriatic drug monomethyl fumarate, which is known to also induce a flushing reaction (24), was recently shown to activate GPR109A (25), which suggests that this receptor can also mediate antiinflammatory effects in the skin.

Given the obvious clinical relevance of GPR109A activation in the skin, we sought to better understand the mechanisms underlying GPR109A-mediated flushing. Using various genetic and pharmacological tools, we demonstrated that keratinocytes were critically involved in the flush reaction and that GPR109A-mediated flushing resulted from 2 distinct mechanisms based on the activation of Langerhans cells and of keratinocytes.

Results

Keratinocytes express GPR109A. To analyze the expression of GPR109A in detail, we generated a BAC-based transgenic mouse line expressing the monomeric red fluorescent protein (mRFP) under the control of the murine *Gpr109a* gene promoter

Conflict of interest: The authors have declared that no conflict of interest exists.
Citation for this article: *J Clin Invest* doi:10.1172/JCI42273.

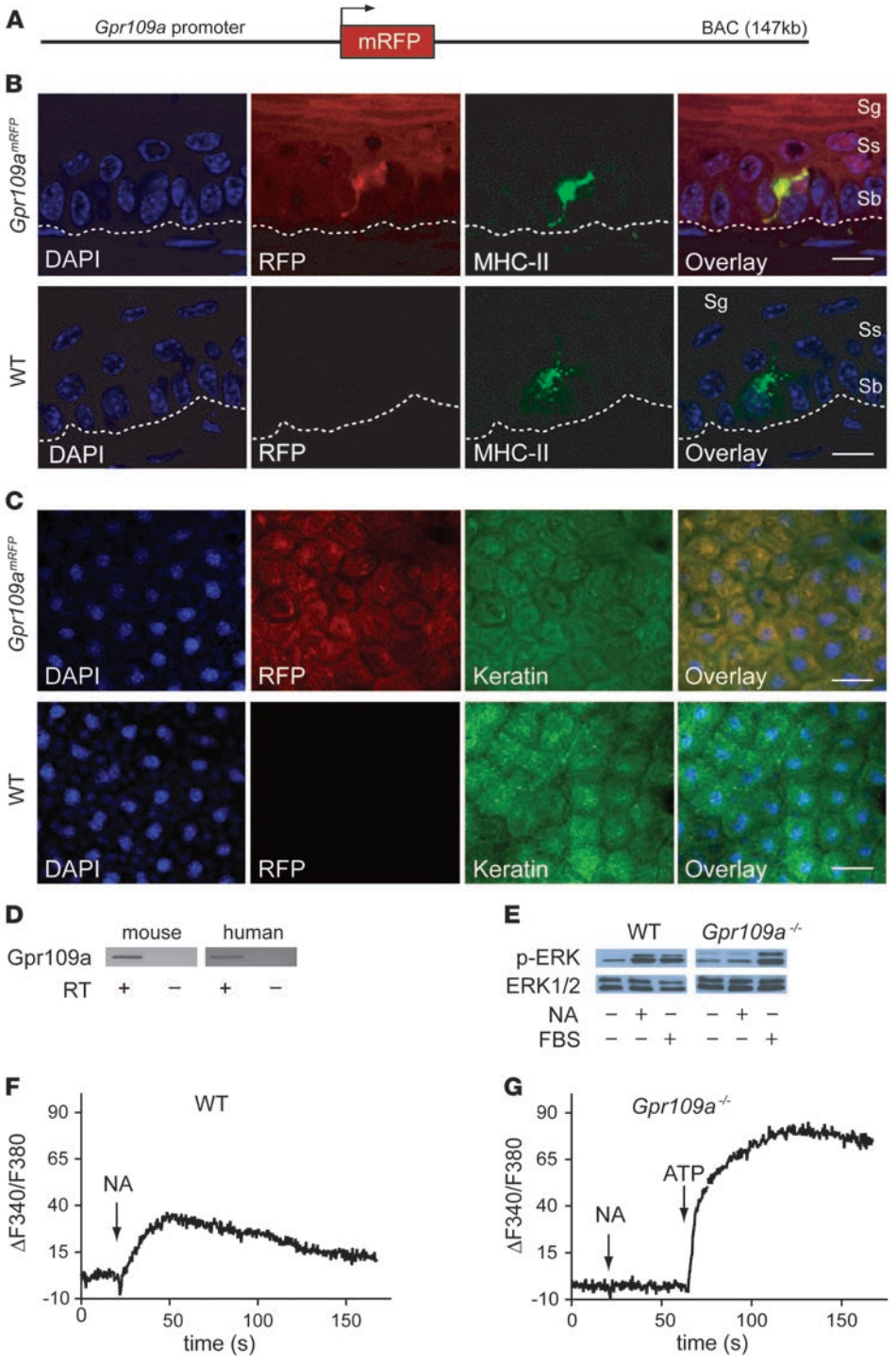

Figure 1
Keratinocytes express GPR109A. (**A**) Scheme of the *Gpr109a* reporter BAC transgene. (**B** and **C**) Gpr109a expression in the epidermis. Shown are sections through the epidermis (**B**) and en face views of the epidermis (**C**) from WT and *Gpr109a*^{mRFP} mice. Cell nuclei were stained with DAPI, and keratinocytes and Langerhans cells were visualized by immunofluorescence labeling with antibodies directed against MHC-II (**B**) and cytokeratin (**C**). mRFP fluorescence was detected in parallel to visualize GPR109A expression. Dotted line denotes the basal membrane. Sb, stratum basale; Sg, stratum granulosum; Ss, stratum spinosum. Scale bars: 10 μm (**B**); 20 μm (**C**). (**D**) RT-PCR to analyze Gpr109a expression in human and mouse keratinocytes. The cDNA synthesis reaction was performed in the absence or presence of RT. (**E**) Effects of 100 μM nicotinic acid (NA) and 10% FBS on ERK1/2 phosphorylation in keratinocytes prepared from WT or *Gpr109a*$^{-/-}$ mice, analyzed with an antibody recognizing phosphorylated ERK1/2. In parallel, the total amount of ERK1/2 was determined. (**F** and **G**) Effect of 100 μM NA on free $[Ca^{2+}]_i$ in Fura-2–loaded keratinocytes from WT (**F**) and *Gpr109a*$^{-/-}$ (**G**) mice. ATP (100 μM) was applied as a positive control.

(*Gpr109a*^{mRFP} mice; Figure 1A). In 5 independent transgenic lines, we found expression of mRFP in adipocytes and in various tissues containing immune cells, such as spleen or BM (data not shown and Supplemental Figure 1; supplemental material available online with this article; doi:10.1172/JCI42273DS1), reflecting the known expression pattern of GPR109A. In skin sections, we observed mRFP expression in epidermal Langerhans cells using confocal fluorescence microscopy (Figure 1B). In addition to Langerhans cells, keratinocytes also showed mRFP expression, albeit at levels lower than those in Langerhans cells (Figure 1, B and C, and Supplemental Figure 2). To verify that keratinocytes express GPR109A, we performed RT-PCR on mRNA of human and mouse keratinocytes. The purity of the keratinocyte mRNA was verified by the absence of any Langerhans cell–specific langerin mRNAs (Supplemental Figure 3). GPR109A expression, in contrast, was seen in both mouse and human keratinocytes (Figure 1D).

We then tested whether GPR109A expressed by keratinocytes is functionally active. Nicotinic acid induced activation of ERK in

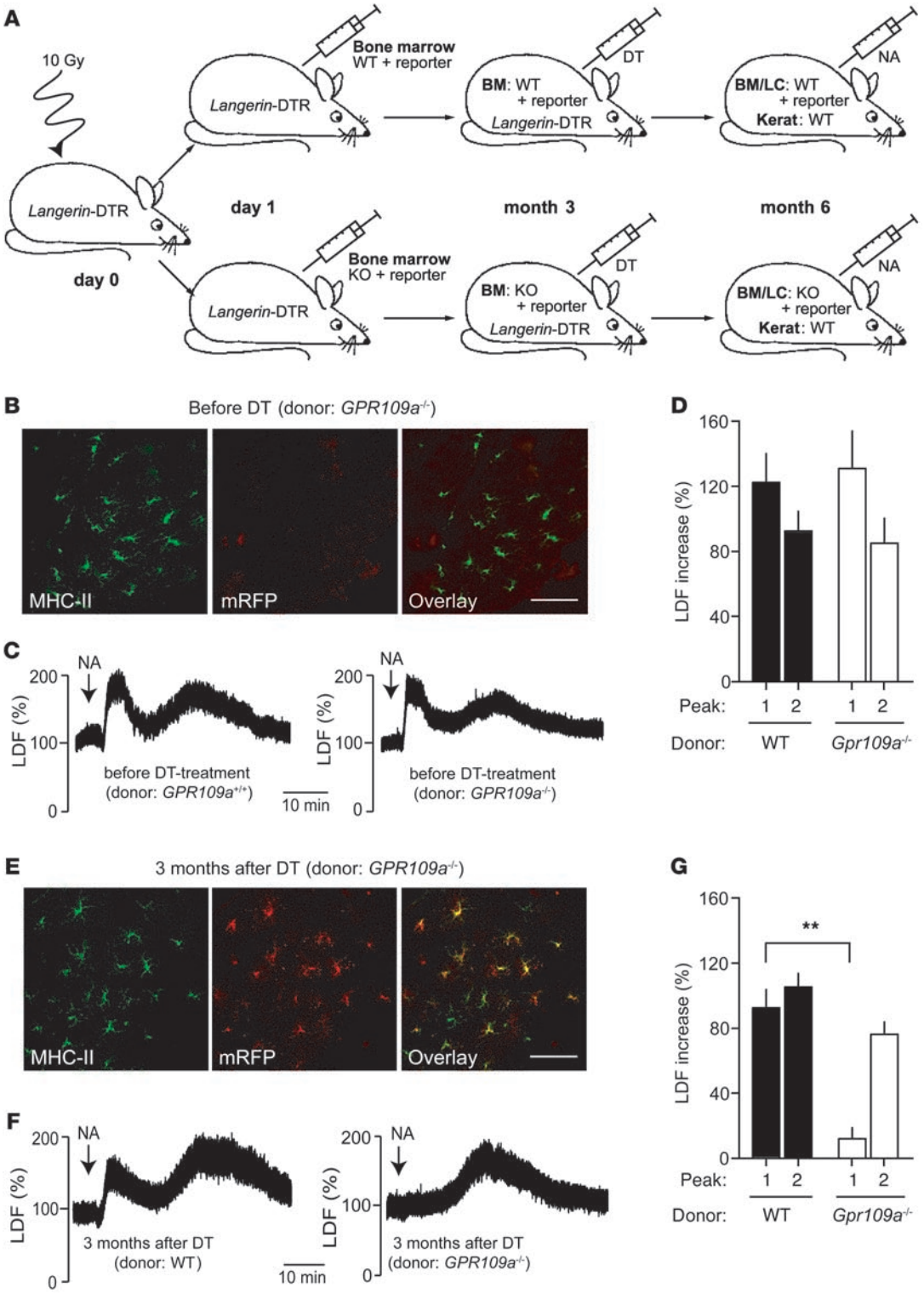

Figure 2

GPR109A expressed by Langerhans cells mediates only the early phase of nicotinic acid–induced flushing. (**A**) Experimental scheme. At 1 day after irradiation, *Langerin*-DTR mice were transplanted with BM from WT or *Gpr109a*$^{-/-}$ mice carrying in both cases *Gpr109a*^{mRFP} (reporter). At 3 months after transplantation, both groups were treated with DT, and 3 months later, nicotinic acid–induced flushing was evaluated. LC, Langerhans cells; kerat, keratinocytes. (**B**) Fluorescence image of epidermal sheet from transplanted animals before DT treatment stained with an anti–MHC-II antibody and analyzed for mRFP expression. (**C** and **D**) Nicotinic acid (250 μg/g) induced flushing in both experimental groups before DT treatment. (**E**) Fluorescent images of epidermal sheets of transplanted animals stained with anti–MHC-II antibodies and analyzed for mRFP expression 3 months after DT treatment. (**F** and **G**) Effect of nicotinic acid on flushing in mice transplanted with WT and *Gpr109a*$^{-/-}$ BM 3 months after DT treatment. Scale bars: 20 μm. Data are representative of at least 3 independent experiments. Results in **D** and **G** are mean ± SEM ($n \geq 6$). $^{**}P \leq 0.01$.

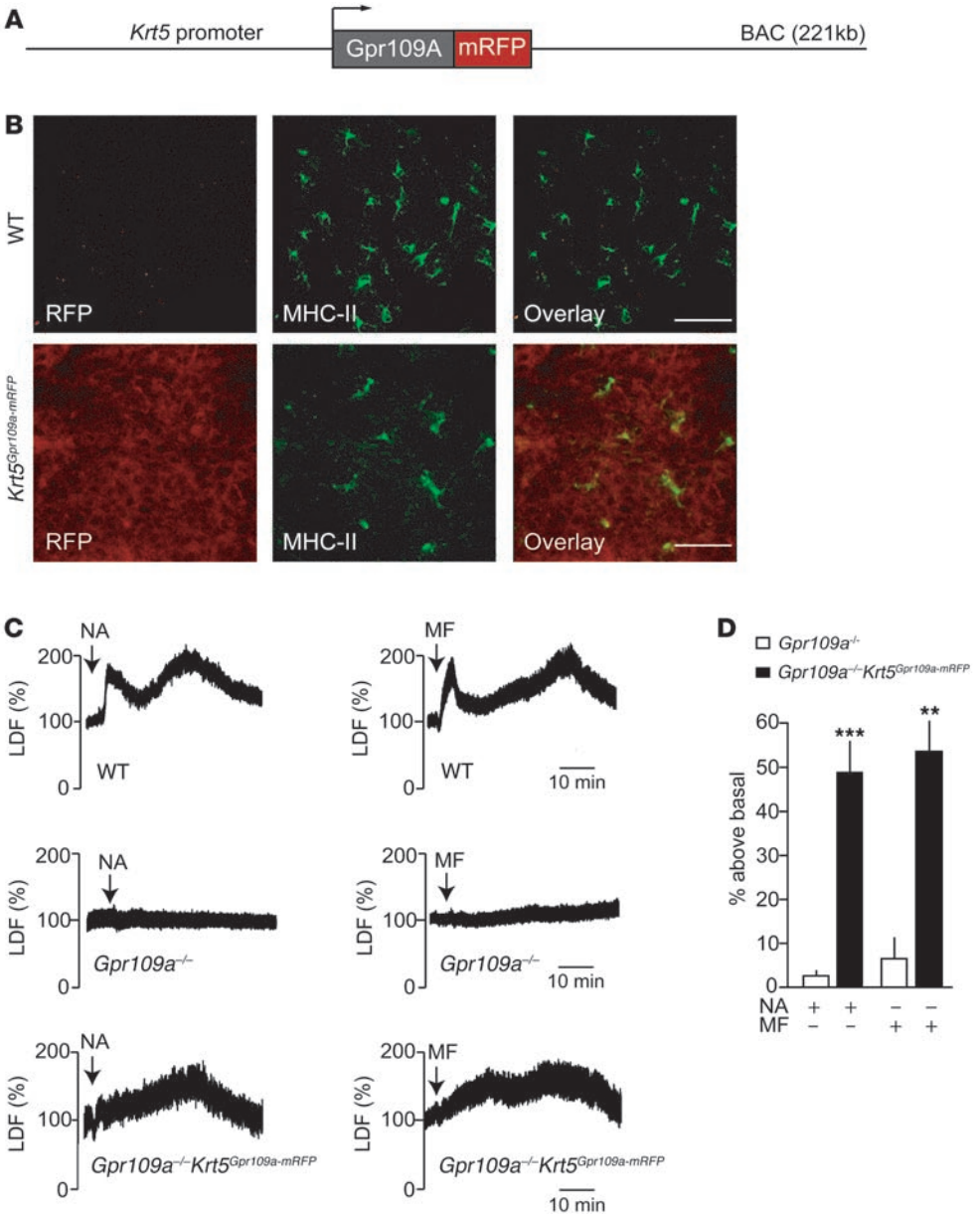

Figure 3
Expression of GPR109A in keratinocytes is sufficient to mediate the late phase of nicotinic acid–induced flushing. (**A**) Scheme of the *Krt5*$^{Gpr109a\text{-}mRFP}$ BAC transgene. (**B**) Fluorescence image of epidermal sheets prepared from WT and *Krt5*$^{Gpr109a\text{-}mRFP}$ mice. Shown are en face views of epidermal sheets stained with anti–MHC-II antibodies and analyzed for expression of mRFP. Scale bars: 25 μm. (**C** and **D**) Effect of 250 μg/g nicotinic acid and 10 μg/g monomethyl fumarate (MF) on flushing in WT, *Gpr109a*$^{-/-}$, and *Gpr109a*$^{-/-}$*Krt5*$^{Gpr109a\text{-}mRFP}$ mice. The experiments shown are representative of at least 9 experiments. Data in **D** show the evaluation of the late phase of flushing (second peak) and are presented as mean ± SEM ($n > 9$). $^{**}P \leq 0.01$, $^{***}P \leq 0.001$ versus *Gpr109a*$^{-/-}$.

WT keratinocytes, but not in *Gpr109a*$^{-/-}$ keratinocytes, whereas both responded to FBS (Figure 1E). Keratinocytes from WT and *Gpr109a*$^{-/-}$ mice were loaded with Fura-2 and exposed to 100 μM nicotinic acid. WT keratinocytes responded with a transient increase in free intracellular calcium concentration ($[Ca^{2+}]_i$), whereas *Gpr109a*$^{-/-}$ keratinocytes were unresponsive to nicotinic acid, but still able to respond to ATP (Figure 1, F and G).

GPR109A expressed by Langerhans cells mediates only the early phase of GPR109A-dependent flushing. The expression of GPR109A in keratinocytes suggests that activation of GPR109A on keratinocytes is involved in the nicotinic acid–induced cutaneous flushing reaction. To be able to study the contribution of keratinocytes to nicotinic acid–induced flushing, we generated BM chimeras by transplanting WT or *Gpr109a*$^{-/-}$ BM onto irradiated WT mice. To promote the replacement of resident epidermal Langerhans cells by cells derived from the transplanted BM, we used transgenic animals expressing the human diphtheria toxin receptor under the control of the langerin promoter as recipients (*Langerin*-DTR mice; Figure 2A). In these animals, treatment with diphtheria toxin (DT) results in the ablation of Langerhans cells of the recipient, but not of Langerhans cells derived from the transplanted BM (26). To track the expression of GPR109A in the transplanted BM and the cells derived from it, the donor animals carried the *Gpr109a*^{mRFP} reporter transgene (Figure 2A). At 3 months after transplantation, hardly any *Gpr109a*^{mRFP}-positive Langerhans cells were detected in the epidermis of transplanted mice, which indicates that the Langerhans cells of the recipient were not yet replaced by cells from the BM (Figure 2B). As expected, the nicotinic acid–induced flushing response determined by laser Doppler flowmetry was not changed compared with WT animals, and there were no differences in the flushing response between mice transplanted with WT and *Gpr109a*$^{-/-}$

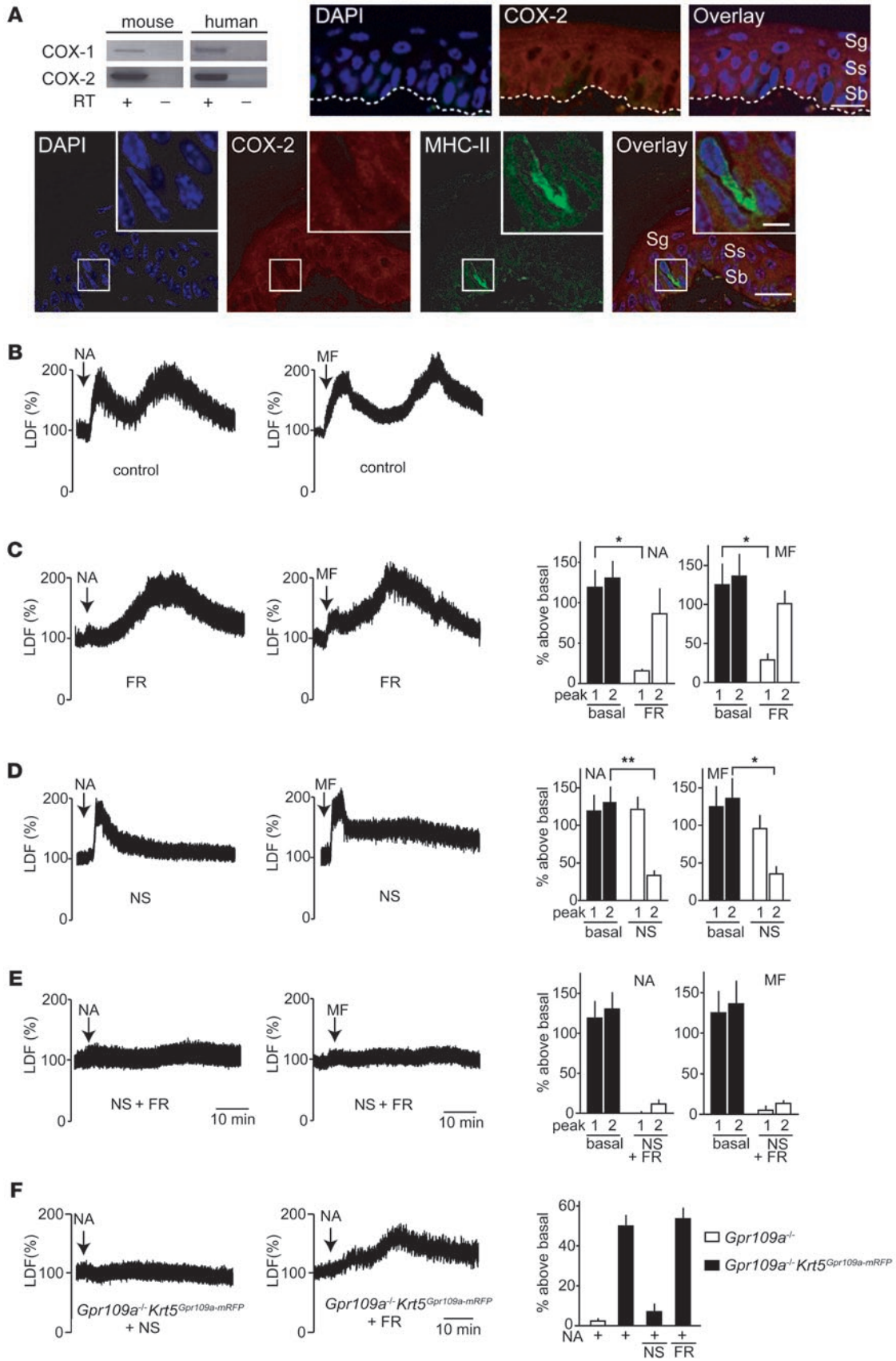
A
mouse
human
COX-1
COX-2
RT + − + −
DAPI
COX-2
Overlay
Sg
Ss
Sb
DAPI
COX-2
MHC-II
Overlay
Sg
Ss
Sb
B
NA
MF
LDF (%)
200
100
0
control
control
C
NA
MF
FR
FR
% above basal
150
100
50
0
peak 1 2
basal
FR
*
D
NA
MF
NS
NS
**
*
basal
NS
E
NA
MF
NS + FR
NS + FR
10 min
basal
NS + FR
F
LDF(%)
Gpr109a-/- Krt5Gpr109a-mRFP + NS
Gpr109a-/- Krt5Gpr109a-mRFP + FR
10 min
60
40
20
0
Gpr109a-/-
Gpr109a-/- Krt5Gpr109a-mRFP
NA + + + +
NS FR

Figure 4
Roles of COX-1 and COX-2 in GPR109A-mediated flushing. (**A**) RT-PCR to determine COX-1 and COX-2 expression in human and mouse keratinocytes, and analysis of COX-2 expression in the epidermis. The cDNA synthesis reaction was performed in the absence or presence of RT. Shown are transversal sections of tail epidermis stained with DAPI and with antibodies specific to COX-2 and MHC-II. Dotted line denotes the basal membrane. Scale bars: 10 μm; 2 μm (insets). (**B**–**F**) Flushing responses induced by 250 μg/g nicotinic acid and 10 μg/g monomethyl fumarate in WT mice pretreated 45 minutes prior to the injection of nicotinic acid or monomethyl fumarate in the absence (**B**) or presence of 5 μg/g FR122047 (FR; **C**), 10 μg/g NS398 (NS; **D**), or pretreated with both inhibitors (**E**), or in *GPR109A*$^{-/-}$*Krt5*$^{Gpr109a\text{-}mRFP}$ mice pretreated with the same doses of FR122047 or NS398 (**F**). Shown are representative traces as well as quantification of at least 4 experiments. Data are mean ± SEM ($n \geq 4$). $^{*}P \leq 0.05$; $^{**}P \leq 0.01$.

BM (Figure 2, C and D). At 3 months after DT treatment of mice (i.e., 6 months after BM transplantation), most Langerhans cells were mRFP positive (Figure 2E), indicative of successful quantitative exchange of the Langerhans cell population in the skin of transplanted animals. Mice with WT Langerhans cells showed a normal flushing response (Figure 2, F and G). Surprisingly, animals with *Gpr109a*$^{-/-}$ Langerhans cells lacked only the first peak of the flushing reaction; the second peak was unaltered (Figure 2, F and G). This suggests that GPR109A expressed on Langerhans cells is required for the initial phase of the flushing reaction, whereas GPR109A expressed on keratinocytes may mediate the late phase of the flushing response.

Expression of GPR109A by keratinocytes is sufficient to mediate the late phase of flushing. To study whether expression of GPR109A on keratinocytes is sufficient for the induction of the late phase of nicotinic acid–induced flushing, we generated mice expressing a GPR109A-mRFP fusion protein under the control of the *Krt5* promoter (*Krt5*$^{Gpr109a\text{-}mRFP}$ mice; Figure 3A). The GPR109A-mRFP fusion protein was functionally active when tested in vitro and mediated nicotinic acid–induced Ca^{2+} transients similar to those mediated by the WT receptor (Supplemental Figure 4). Expression of the GPR109A-mRFP protein in keratinocytes was verified by confocal immunofluorescence microscopy (Figure 3B). Staining of epidermal sheets with anti–MHC-II antibodies showed that Langerhans cells did not express the GPR109A-mRFP fusion protein. No expression of the fusion protein was observed in other organs like dermis, blood vessels, spleen, liver, or adipose tissue (data not shown). We then crossed *Krt5*$^{GPR109A\text{-}mRFP}$ mice with animals lacking GPR109A, generating *Gpr109a*$^{-/-}$*Krt5*$^{GPR109A\text{-}mRFP}$ mice, which express GPR109A only in keratinocytes. Nicotinic acid induced an increase in free $[Ca^{2+}]_i$ and in the phosphorylation of ERK1/2 with similar efficacy in keratinocytes prepared from *Gpr109a*$^{-/-}$*Krt5*$^{Gpr109a\text{-}mRFP}$ and WT mice (Supplemental Figure 5 and Figure 1), which indicates that the transgenically expressed fusion protein was functionally equivalent to GPR109A in WT cells. Since monomethyl fumarate was recently shown to be an agonist of GPR109A (25), we tested both nicotinic acid and monomethyl fumarate for their ability to induce flushing in WT, *Gpr109a*$^{-/-}$, and *Gpr109a*$^{-/-}$*Krt5*$^{GPR109A\text{-}mRFP}$ mice (Figure 3C). The typical biphasic flushing reaction seen in WT mice in response to nicotinic acid and monomethyl fumarate was absent in mice lacking GPR109A. However, both GPR109A agonists induced a delayed transient flushing response in *GPR109A*$^{-/-}$*Krt5*$^{GPR109A\text{-}mRFP}$ animals (Figure 3, C and D). In its time course and intensity, this delayed and transient flush resembled the second phase (i.e., second peak) of the nicotinic acid–induced flushing response seen in WT animals. This clearly indicates that activation of GPR109A on keratinocytes is sufficient to induce the late phase of the flushing reaction, but does not mimic the early, initial flushing response.

Differential roles of COX-1 and COX-2 in GPR109A-mediated flushing. We then further analyzed potential mechanisms underlying the late phase of the nicotinic acid– and monomethyl fumarate–induced flushing reaction. Since nicotinic acid–induced flushing has been shown to be strongly reduced by cyclooxygenase inhibitors, we studied expression of cyclooxygenase-1 (COX-1) and COX-2 in mouse and human keratinocytes. RT-PCR clearly showed that both enzymes were expressed in keratinocytes (Figure 4A). Immunostaining with a COX-2–specific antibody confirmed expression of COX-2 in the keratinocyte layer of the epidermis. The specificity of the anti–COX-2 antibody was verified by the absence of any epidermal staining in the skin of COX-2–deficient mice (Supplemental Figure 6). Counterstaining with an anti–MHC-II antibody, which recognizes only Langerhans cells in the epidermis, clearly showed that Langerhans cells, in contrast to keratinocytes, did not express COX-2 (Figure 4A). Treatment of animals with the COX-1 inhibitor FR122047 (27) blocked the initial flush reaction in response to nicotinic acid and monomethyl fumarate compared with untreated animals, but left the late phase unaffected (Figure 4, B and C). Interestingly, when mice were treated with the COX-2 inhibitor NS398 (28), the initial flushing reaction was unaffected, whereas the late phase of nicotinic acid– and monomethyl fumarate–induced flushing was abrogated (Figure 4D). Pretreatment of mice with FR122047 and NS398 combined fully blocked the flush response (Figure 4E). In *GPR109A*$^{-/-}$*Krt5*$^{Gpr109a\text{-}mRFP}$ mice, NS398 fully blocked nicotinic acid–induced flushing, whereas FR122047 was without effect (Figure 4F). These data confirmed that GPR109A-mediated flushing involves prostanoids. In addition, the data indicated that COX-1 activity is required for the initial phase of the flushing reaction, which is mediated by Langerhans cells, whereas the late phase requires COX-2. This clearly supports the notion that the early and late phases of GPR109A-mediated flushing involve different mechanisms.

Keratinocytes produce PGE_2 via COX-2 in response to GPR109A activation. Since activation of GPR109A on keratinocytes was sufficient to induce the late phase of flushing, and since this phase was sensitive to COX-2 inhibitors, we studied expression of prostanoid synthases in keratinocytes. RT-PCR on mouse and human keratinocyte mRNA showed that the PGE_2 synthases mPGES-1, mPGES-2, and cPGES and the PGD_2 synthases PGDS-L and PGDS-H were expressed in keratinocytes (Figure 5A). Therefore, we tested whether mouse and human keratinocytes produce PGD_2 and PGE_2 in response to nicotinic acid in vitro. Incubation of isolated mouse and human keratinocytes with nicotinic acid or monomethyl fumarate led to the formation of PGE_2 (Figure 5, B–D), whereas no increase in PGD_2 formation was observed (Supplemental Figure 7). In keratinocytes from *Gpr109a*$^{-/-}$ mice, nicotinic acid and monomethyl fumarate were without effect (Figure 5C). In both human and mouse keratinocytes, the effects of GPR109A agonists on PGE_2 formation were completely blocked by NS398, whereas FR122047 was without effect (Figure 5, C and D). These data indicate that the stimulation of COX-2 dependent PGE_2 formation in keratinocytes underlies the late phase of nicotinic acid– and monomethyl fumarate–induced flushing.

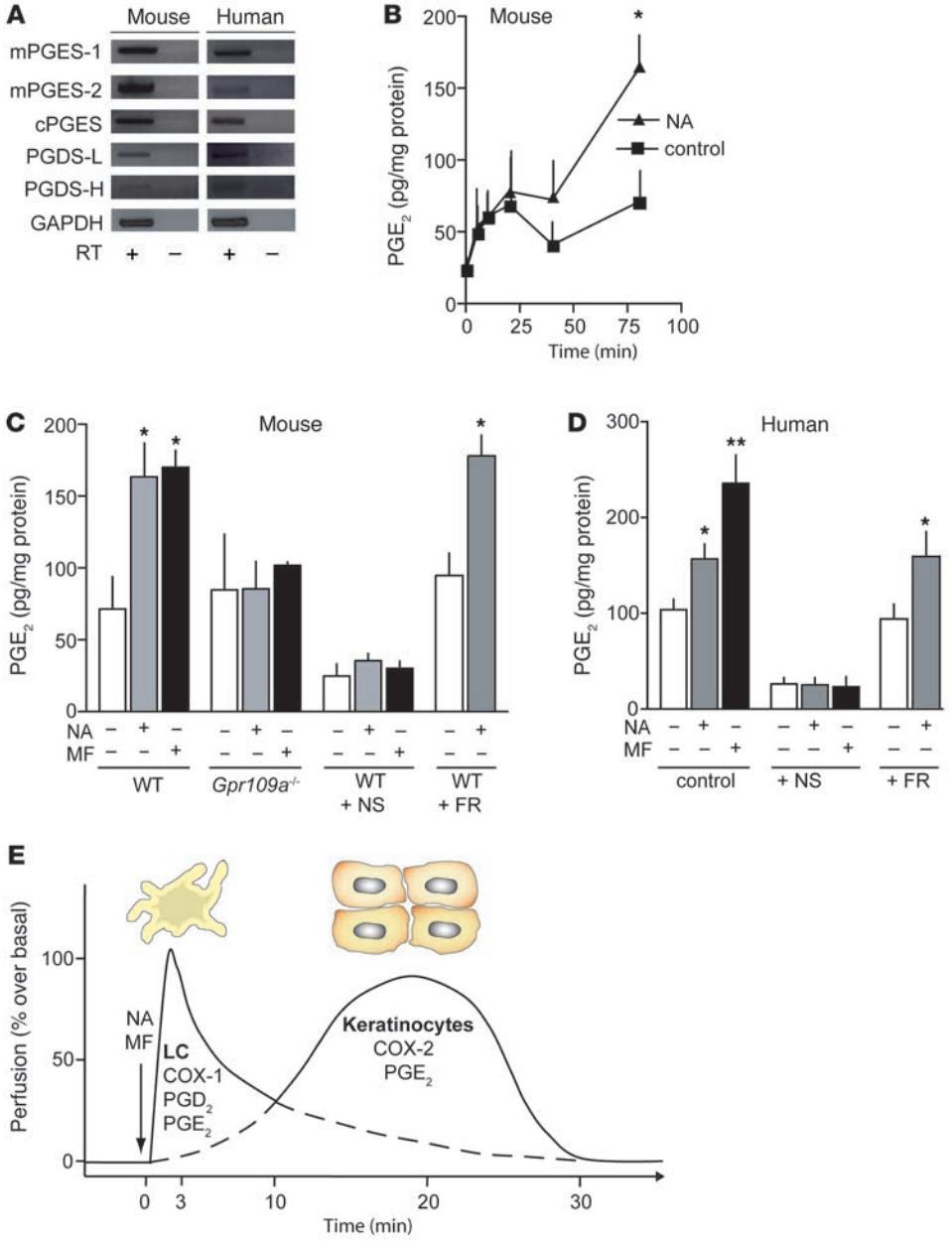

Figure 5
GPR109A-mediated stimulation of prostanoid release from keratinocytes. (**A**) RT-PCR to determine the expression of PGE_2 and PGD_2 synthases as well as GAPDH in human and mouse keratinocytes. The cDNA synthesis reaction was performed in the absence or presence of RT. (**B**) Effect of nicotinic acid on the release of PGE_2 from mouse keratinocytes, shown for increasing time periods. (**C** and **D**) Effect of nicotinic acid and monomethyl fumarate on the release of PGE_2 from mouse (**C**) and human keratinocytes (**D**). Mouse keratinocytes were prepared from WT or *Gpr109a*$^{-/-}$ mice. Keratinocytes were left untreated or were pretreated with NS398 (10 μM) or FR122047 (1 μM). Nicotinic acid and monomethyl fumarate were applied at a concentration of 500 μM. Data shown are mean ± SEM ($n \geq 4$). $^*P \leq 0.05$, $^{**}P \leq 0.01$ versus samples without agonist. (**E**) Proposed model for the local mechanisms underlying GPR109A-mediated flushing. Application of GPR109A agonists induces a biphasic increase in dermal blood flow, which results from activation of GPR109A on Langerhans cells and keratinocytes. The first phase is induced via activation of GPR109A on Langerhans cells, and GPR109A on keratinocytes is responsible for the late phase of the response. Whereas Langerhans cell–mediated flushing involves COX-1, PGD_2, and PGE_2, keratinocyte-mediated late-phase flushing involves COX-2 and PGE_2.

Discussion

A cutaneous flushing reaction is a common effect of clinically applied GPR109A receptor agonists, like the antidyslipidemic drugs nicotinic acid and acipimox (4, 7, 29) or the antipsoriatic drug monomethyl fumarate (24, 25). Although this epidermal reaction may be a direct reflection of the wanted effects of monomethyl fumarate, it is the most troublesome unwanted effect of nicotinic acid and related antidyslipidemic drugs. Since both wanted and unwanted effects of nicotinic acid appear to be mediated by GPR109A (12, 18, 30), it will be difficult to dissociate wanted and unwanted effects on the basis of GPR109A agonism. The use of partial agonists or of agonists that activate GPR109A in a β-arrestin–independent manner has been suggested to preferentially induce wanted effects mediated by GPR109A (31, 32). Alternatively, GPR109A-mediated flushing can be inhibited by interfering with downstream signaling events specific to the unwanted effects, a strategy requiring a full understanding of the mechanism underlying nicotinic acid–induced flushing. An improved mechanistic insight into the GPR109A-mediated flushing reaction will also be important to understand the beneficial effects of monomethyl fumarate. Although evidence has been provided that epidermal Langerhans cells and prostanoids, such as PGD_2 and PGE_2, are involved in the GPR109A-dependent flush reaction, the mechanisms underlying the flush phenomenon are still poorly understood. Here we provided evidence that flushing involves not only Langerhans cells, but also keratinocytes, and that it is mediated by 2 distinct cellular pathways involving activation of GPR109A on Langerhans cells and on keratinocytes as well as by distinct prostanoid-mediated downstream signaling processes.

The receptor GPR109A is not only expressed by adipocytes, but also by various immune cells, such as macrophages, neutrophils, and epidermal Langerhans cells, but not by lymphocytes (23, 25, 33, 34). Whether GPR109A is expressed by keratinocytes has been unclear. Expression analyses on the level of mRNA showed GPR109A expression in primary human keratinocytes (23, 25). However, immunohistochemistry failed to demonstrate GPR109A expression in keratinocytes (23). In the present study, we confirmed the presence of GPR109A mRNA in primary mouse and human keratinocytes. In addition, we provided evidence for GPR109A expression in keratinocytes using a GPR109A expression reporter mouse line as well as by demonstrating nicotinic acid's effects on WT, but not *Gpr109a*$^{-/-}$, keratinocytes. The *Gpr109a*^{mRFP} reporter mouse showed that, compared with Langerhans cells, GPR109A expression levels were lower in keratinocytes, a finding that may explain the difficulty in detecting GPR109A expression by immunohistochemistry on keratinocytes.

Our data strongly indicate that GPR109A on keratinocytes is involved in the late phase of flushing induced by nicotinic acid or monomethyl fumarate and that the late phase of the flushing reaction can be induced in the absence of WT Langerhans cells. This is in contrast to earlier data showing that the acute ablation of Langerhans cells by DT strongly reduced the early and late phases of nicotinic acid–induced flushing (22). The contribution of keratinocytes may have been overseen as a result of DT-induced Langerhans cell ablation, which is caused by apoptosis and subsequent removal of apoptotic cells (35, 36), a process involving the whole Langerhans cell compartment of the epidermis. Such a profound reaction of the epidermal layer of the skin is likely to affect epidermal functions and lead to transient unresponsiveness with regard to nicotinic acid–induced keratinocyte-dependent flushing. In contrast to the experiment described previously (22), we determined nicotinic acid–induced flushing in the present study 3 months after DT treatment, when ablated Langerhans cells were already replaced by new cells.

The abrogation of the Langerhans cell–mediated early phase of nicotinic acid– and monomethyl fumarate–induced flushing by a COX-1–selective blocker is in line with earlier genetic studies showing a severely reduced flushing reaction in COX-1–deficient mice (12). However, the flush response that remained in COX-1–deficient mice was smaller than the remaining response in animals acutely treated with a COX-1 inhibitor. This may be due to compensatory changes taking place in constitutive COX-1–deficient animals. Our data revealed an important role for COX-2 in mediating the keratinocyte-dependent late phase of the flush reaction. COX-2 has previously been shown to be expressed in keratinocytes and to mediate acute reactions to UVB light (37–40), which, interestingly, share many properties with the GPR109A-mediated flush reaction, such as vasodilation and a burning sensation. PGE_2 is the major prostanoid produced by keratinocytes (41, 42), and epidermal PGE_2 generation has been shown to induce vasodilation (43). Langerhans cells, in contrast, also produce considerable amounts of PGD_2 (23, 44, 45). The involvement of PGE_2 in the keratinocyte-mediated late phase of GPR109A-dependent flushing is consistent with the observation that in mice lacking the PGD_2 receptor DP_1, only the first phase of the flush was reduced, whereas the lack of the PGE_2 receptors EP_2 and EP_4 inhibited the early and late phases (12). The involvement of PGE_2 in the keratinocyte-dependent late phase of flushing explains the remaining flush response seen in animals and humans after blockade of DP_1 (18, 19). The fact that oral administration of 325 mg aspirin is not able to reduce the residual flushing seen when nicotinic acid is combined with the DP_1 receptor antagonist laropiprant (46) does not contradict the role of PGE_2 mainly produced via COX-2 in the flushing reaction, since 325 mg aspirin given orally may not lead to systemic aspirin concentrations sufficiently high to block COX-2 in keratinocytes and therefore block the second phase of flushing (47–49).

It is currently not clear why the Langerhans cell–mediated part of the nicotinic acid–induced flush reaction starts rapidly after nicotinic acid application, whereas the keratinocyte-mediated part sets in with some delay. Given the higher expression level of GPR109A in Langerhans cells compared with keratinocytes and the different intracellular mechanisms mediating prostanoid formation in both cell types, the time required to reach sufficient prostanoid levels to induce flushing may be shorter in Langerhans cells than in keratinocytes. It is also conceivable that prostanoids released in response to GPR109A agonists from keratinocytes require a longer time period to elicit their effects on dermal blood vessels compared with prostanoids released from Langerhans cells.

The presence of GPR109A in Langerhans cells and keratinocytes and the marked epidermal and dermal effects resulting from GPR109A activation raise the question whether this receptor system, besides its pharmacological role, has any physiological or pathophysiological significance. It is tempting to speculate that GPR109A-mediated prostanoid formation in Langerhans cells and keratinocytes underlies some of the many forms of skin reaction in which alteration or traumata in the epidermis results in dermal vasodilation and tingling or burning sensations. The fact that monomethyl fumarate is an agonist of GPR109A suggests that it exerts its beneficial effects via GPR109A by influencing keratinocytes and Langerhans cells, which are intimately involved in the pathophysiology of psoriasis (50). It will be interesting to further explore the potential physiological and pathophysiological role of GPR109A-mediated cellular effects in the epidermis, a task that will be facilitated by synthetic GPR109A agonists and antagonists currently under development.

Here we showed that nicotinic acid– and monomethyl fumarate–induced flushing resulted from 2 GPR109A-mediated mechanisms, involving Langerhans cells and keratinocytes as well as different prostanoid-forming enzymes (Figure 5E). These data will help to further improve flush-reducing strategies in patients taking GPR109A agonists like nicotinic acid by combined inhibition of COX-1 and COX-2 or PGD_2 and PGE_2 formation or activity. In addition, our present data shed light on the mechanism of action of the antipsoriatic drug monomethyl fumarate and suggest that GPR109A expressed on epidermal cells mediates antipsoriatic effects.

Methods

Reagents and antibodies. Nicotinic acid, monomethyl fumarate, and ATP were from Sigma-Aldrich. NS398 was from Cayman Chemical, and FR122047 was from Tocris. Anti–MHC-II–IA/IE antibodies were from Becton Dickinson, anti–pan-cytokeratin and anti–COX-2 antibodies were from Santa Cruz Biotechnology. Anti–phospho-ERK1/2 and anti-ERK1/2 antibodies were from Cell Signaling.

Mice. Experiments were carried out in WT and genetically altered adult mice (body weight 20–30 g) on a C57BL/6 background. When testing knockout animals, WT littermates served as controls. Mice were housed in temperature-controlled facilities on a 12-hour light/12-hour dark cycle with food and water ad libitum. All procedures of animal care and use in this study were approved by Regierungspräsidium Karlsruhe (Karlsruhe, Germany).

Gpr109a$^{-/-}$ and *Langerin*-DTR mice have been described previously (22, 26, 30). To generate a Gpr109a expression reporter mouse line (*Gpr109a*^{mRFP}), the coding sequence of the mouse *Gpr109a* gene carried by the BAC RP23-91D24 was replaced by a cassette consisting of the mRFP followed by a polyadenylation signal from bovine growth hormone and a module containing the β-lactamase gene flanked by frt sites using RecE/RecT recombination, as described previously (51, 52). To generate the *Krt5*$^{Gpr109a\text{-}mRFP}$ mouse line, a cassette containing the coding sequence of Gpr109a followed in frame by that of mRFP and by a polyadenylation signal together with the β-lactamase gene flanked by frt sites was introduced into the ATG of the mouse *Krt5* gene carried by a BAC (RP23-437J8) using RecE/RecT recombination. Correct recombinants were verified by Southern blotting, PCR, and sequencing. After FLP-mediated excision of the β-lactamase gene, the recombined BACs were injected into pronuclei of FvB/N oocytes. Transgenic offspring was analyzed for BAC insertion by genomic PCR. At least 5 different founders were used to generate *Gpr109a*^{mRFP} and *Krt5*$^{Gpr109a\text{-}mRFP}$ mouse lines. Expression of the transgenes was determined by fluorescence microscopy of whole organs or 5- to 20-μm cryosections of various tissues. All lines generated with the same transgene showed a comparable expression pattern for mRFP. Animals were kept on a C57BL/6 background.

Flushing. Flushing was determined as described previously (12). Briefly, mice were anesthetized by i.p. injection of 60 mg/kg pentobarbital (Narcoren; Merial) and placed on their left sides on a controlled heating pad (TKM-0902; Föhr Medical Instruments). A small straight laser Doppler probe (no. 407; Perimed) was attached to the dorsal surface of the right ear over a first-order branch of the main ear artery. Laser Doppler flux (LDF) was continuously recorded by a PeriFlux 5001 LD monitor (Perimed) connected to a PC via the MP100 system (Biopac Systems Inc.). Recordings were analyzed offline with AcqKnowledge 3.7.3 software (Biopac Systems Inc.). After a 10-minute stabilization period, nicotinic acid and monomethyl fumarate were applied at doses of 250 and 10 μg/g body weight, respectively, in a volume of 20 μl/g. None of the vehicles induced any change in ear blood flow, systemic blood pressure, or heart rate in control experiments (data not shown). In all experiments, baseline LDF was determined prior to injection of the tested compound. Nicotinic acid and monomethyl fumarate induced a biphasic flush, and therefore the maximal LDF values of the first and second flushing were determined and expressed as percentages of the baseline flow. All data are presented as mean ± SEM. At least 1 week was allowed for recovery between experiments in the same animal.

BM transplantation. BM transplantation was performed as described previously (53). BM was obtained aseptically from femurs and tibias of *Gpr109a*^{mRFP} or *Gpr109a*^{mRFP}*Gpr109a*$^{-/-}$ mice after euthanizing animals by cervical dislocation. Unfractionated BM cells (5×10^6) were resuspended in sterile PBS and transplanted by tail vein infusion into lethally irradiated (10 Gy) *Langerin*-DTR transgenic recipients 1 day after irradiation.

DT treatment. After control experiments, the BM-transplanted *Langerin*-DTR transgenic animals were treated with 16 ng/g DT, as described previously (22). DT was injected i.p. twice within 24 hours before retesting of the flushing responses 3 months later.

Immunostaining of epidermal sheets and skin sections. Mouse ears were dissected and split into ventral and dorsal sheets. After 1 hour digestion in serum-free RPMI1640 containing 10 mM EDTA, the epidermis was removed from the dermis using fine forceps and was fixed on ice for 1 hour in 4% paraformaldehyde/PBS. After permeabilization with 0.2% Triton/PBS for 10 minutes at 25°C and 2 washes with PBS for 10 minutes, the epidermal sheets were incubated with 10% goat serum for 30 minutes. FITC-labeled anti–MHC-II–IA/IE and anti–pan-cytokeratin antibodies were incubated in 10% goat serum/PBS with epidermal sheets overnight at 4°C on a rotator. Anti-keratin antibodies were then stained with FITC-labeled secondary antibodies. After washing, epidermal sheets were mounted and analyzed by fluorescence microscopy. Cryosections of tail tissue (10–14 μm) were fixed for 10 minutes with cold acetone and incubated for 30 minutes in PBS containing 10% goat serum. Sections were incubated overnight with FITC-labeled anti–MHC-II–IA/IE and anti–COX-2 antibodies. Anti–COX-2 antibodies were then stained with TRITC-labeled secondary antibodies. After washing with PBS, sections were mounted and analyzed by fluorescent confocal microscopy (Leica TCS SP3; Leica Microsystems). Skin from COX-2–deficient mice to test for the specificity of the anti–COX-2 antibody was provided by R. Nüsing (University of Frankfurt, Frankfurt, Germany).

Culture of keratinocytes. Normal human epidermal keratinocytes were from PromoCell and were maintained in keratinocyte growth medium (KGM; PromoCell) at 37°C, 5% CO_2. Mouse keratinocytes were isolated as described previously (54). Briefly, mice were euthanized by CO_2, and tail skin was removed and placed in cold (4°C) trypsin/EDTA overnight. The epidermis was removed from skin, and the pooled epidermal sheets were cut in small pieces and dispersed in warm medium. The suspension was filtered through a 100-μm mesh nylon filter (Millipore) and centrifuged at 600 *g* for 10 minutes. The cell pellet was resuspended in medium and plated on collagen-coated plates. Medium was replaced by KGMII the next day and changed every other day.

Determination of ERK activity. Confluent 6-well keratinocyte cultures were starved overnight and incubated with the indicated agents for 5 minutes at 37°C. Cells were washed with ice-cold PBS and lysed in 50 mM Tris-HCl (pH 7.5), 150 mM NaCl, 5 mM EDTA, 1 % (v/v) NP-40, 0.5 % (w/v) sodium desoxycholate, 0.1 % (w/v) SDS, and protease inhibitors. Cell lysates were analyzed by immunoblotting using anti–phospho-ERK1/2 antibodies and an ECL detection system.

Determination of free $[Ca^{2+}]_i$. Mouse keratinocytes were allowed to adhere to collagen-coated glass coverslips (12 mm diameter) and were loaded with Fura-2/AM (3 μM; Invitrogen) for 60 minutes at room temperature. The nonadherent cells were removed by washing with Hanks balanced salt solution containing 2.5 mM Ca^{2+} and 5 mM glucose. Ratiometric calcium signals were recorded using a Zeiss Axiovert 135 microscope, a SensiCam CCD camera (PCO AG), and TILLvisION software version 4.00 (TILL Photonics).

CHO-K1 cells stably transfected with a calcium-sensitive bioluminescent fusion protein consisting of aequorin and green fluorescent protein (55) were seeded in 96-well plates and transfected with indicated cDNAs or control DNA (50 ng/well) using FuGENE 6 reagent (Roche Diagnostics). At 2 days after transfection, cells were loaded with 5 μM coelenterazine h (Biotium) in calcium-free Hanks balanced salt solution containing 10 mM HEPES (pH 7.4) for 3.5 hours at 37°C. At 45 minutes before the experiments, the buffer was replaced with Hanks balanced salt solution containing 1.8 mM $CaCl_2$. Measurements were performed using a luminometer plate reader (Luminoskan Ascent; Thermo Electron Corp.).

RT-PCR. RNA was isolated from keratinocytes with the RNeasy Mini Kit (Qiagen). For RT-PCR, 50 ng to 1 μg total RNA was reverse transcribed. cDNA synthesis was monitored by PCR of a 401-bp fragment of glyceraldehyde 3-phosphate dehydrogenase.

Determination of PGE_2 *and* PGD_2 *formation*. Human and mouse keratinocytes were treated as indicated above. The supernatant was collected, and PGE_2 and PGD_2 concentrations were determined with an ELISA kit according to the manufacturer's instructions (Cayman Chemical). Protein content was determined using Bradford assay and was used to normalize prostanoid concentrations.

Statistics. Statistical analyses of differences between 2 groups was performed by nonparametric, unpaired, 2-tailed Mann-Whitney test. A P value less than 0.05 was considered significant.

Acknowledgments

The authors wish to thank Karin Meyer for expert technical help and Svea Hümmer for excellent secretarial support.

J. Hanson was funded by the Fonds de la Recherche Scientifique-FNRS and by the Humboldt Foundation. This work was supported by grants to S. Offermanns from the German Research Foundation.

Address correspondence to: Stefan Offermanns, Department of Pharmacology, Max-Planck-Institute for Heart and Lung Research, Ludwigstr. 43, 61231 Bad Nauheim, Germany. Phone: 49.6032.705.1201; Fax: 49.6032.705.1204; E-mail: stefan.offermanns@mpi-bn.mpg.de.

Received for publication January 10, 2010, and accepted in revised form May 19, 2010.

Andreas Gille's present address is: CSL Ltd., Clinical and Translational Science Department, Parkville, Victoria, Australia.

1. Canner PL, et al. Fifteen year mortality in Coronary Drug Project patients: long-term benefit with niacin. *J Am Coll Cardiol*. 1986;8(6):1245–1255.
2. Carlson LA. Nicotinic acid: the broad-spectrum lipid drug. A 50th anniversary review. *J Intern Med*. 2005;258(2):94–114.
3. Meyers CD, Kamanna VS, Kashyap ML. Niacin therapy in atherosclerosis. *Curr Opin Lipidol*. 2004;15(6):659–665.
4. Gille A, Bodor ET, Ahmed K, Offermanns S. Nicotinic acid: pharmacological effects and mechanisms of action. *Annu Rev Pharmacol Toxicol*. 2008;48:79–106.
5. Digby JE, Lee JM, Choudhury RP. Nicotinic acid and the prevention of coronary artery disease. *Curr Opin Lipidol*. 2009;20(4):321–326.
6. Brown BG, Zhao XQ. Nicotinic acid, alone and in combinations, for reduction of cardiovascular risk. *Am J Cardiol*. 2008;101(8A):58B–62B.
7. Kamanna VS, Ganji SH, Kashyap ML. The mechanism and mitigation of niacin-induced flushing. *Int J Clin Pract*. 2009;63(9):1369–1377.
8. Davidson MH. Niacin use and cutaneous flushing: mechanisms and strategies for prevention. *Am J Cardiol*. 2008;101(8A):14B–19B.
9. Spies TD, Cooper C, Blankenhorn MA. The use of nicotinic acid in the treatment of pellagra. *JAMA*. 1938;110(9):622–627.
10. Fouts PJ, Helmer OM, Lepkovsky L, Jukes TH. Treatment of human pellegra with nicotinic acid. *Proc Soc Exp Biol Med*. 1937;37:405–407.
11. Goldsmith GA, Cordill S. The vasodilating effects of nicotinic acid (Relation to metabolic rate and body temperature). *Am J Med Sci*. 1943;205(2):204–208.
12. Benyo Z, et al. GPR109A (PUMA-G/HM74A) mediates nicotinic acid-induced flushing. *J Clin Invest*. 2005;115(12):3634–3640.
13. Andersson RG, Aberg G, Brattsand R, Ericsson E, Lundholm L. Studies on the mechanism of flush induced by nicotinic acid. *Acta Pharmacol Toxicol (Copenh)*. 1977;41(1):1–10.
14. Eklund B, Kaijser L, Nowak J, Wennmalm A. Prostaglandins contribute to the vasodilation induced by nicotinic acid. *Prostaglandins*. 1979;17(6):821–830.
15. Kaijser L, Eklund B, Olsson AG, Carlson LA. Dissociation of the effects of nicotinic acid on vasodilatation and lipolysis by a prostaglandin synthesis inhibitor, indomethacin, in man. *Med Biol*. 1979;57(2):114–117.
16. Morrow JD, Parsons WG 3rd, Roberts LJ 2nd. Release of markedly increased quantities of prostaglandin D2 in vivo in humans following the administration of nicotinic acid. *Prostaglandins*. 1989; 38(2):263–274.
17. Stern RH, Spence JD, Freeman DJ, Parbtani A. Tolerance to nicotinic acid flushing. *Clin Pharmacol Ther*. 1991;50(1):66–70.
18. Cheng K, et al. Antagonism of the prostaglandin D2 receptor 1 suppresses nicotinic acid-induced vasodilation in mice and humans. *Proc Natl Acad Sci U S A*. 2006;103(17):6682–6687.
19. Paolini JF, et al. Effects of laropiprant on nicotinic acid-induced flushing in patients with dyslipidemia. *Am J Cardiol*. 2008;101(5):625–630.
20. Bays HE, Ballantyne C. What's the deal with niacin development: is laropiprant add-on therapy a winning strategy to beat a straight flush? *Curr Opin Lipidol*. 2009;20(6):467–476.
21. Perry CM. Extended-release niacin (nicotinic acid)/laropiprant. *Drugs*. 2009;69(12):1665–1679.
22. Benyo Z, Gille A, Bennett CL, Clausen BE, Offermanns S. Nicotinic acid-induced flushing is mediated by activation of epidermal langerhans cells. *Mol Pharmacol*. 2006;70(6):1844–1849.
23. Maciejewski-Lenoir D, Richman JG, Hakak Y, Gaidarov I, Behan DP, Connolly DT. Langerhans cells release prostaglandin D2 in response to nicotinic acid. *J Invest Dermatol*. 2006;126(12):2637–2646.
24. Rostami Yazdi M, Mrowietz U. Fumaric acid esters. *Clin Dermatol*. 2008;26(5):522–526.
25. Tang H, Lu JY, Zheng X, Yang Y, Reagan JD. The psoriasis drug monomethylfumarate is a potent nicotinic acid receptor agonist. *Biochem Biophys Res Commun*. 2008;375(4):562–565.
26. Bennett CL, et al. Inducible ablation of mouse Langerhans cells diminishes but fails to abrogate contact hypersensitivity. *J Cell Biol*. 2005;169(4):569–576.
27. Ochi T, Motoyama Y, Goto T. The analgesic effect profile of FR122047, a selective cyclooxygenase-1 inhibitor, in chemical nociceptive models. *Eur J Pharmacol*. 2000;391(1–2):49–54.
28. Futaki N, Takahashi S, Yokoyama M, Arai I, Higuchi S, Otomo S. NS-398, a new anti-inflammatory agent, selectively inhibits prostaglandin G/H synthase/cyclooxygenase (COX-2) activity in vitro. *Prostaglandins*. 1994;47(1):55–59.
29. Edlund A, Musatti L, Wennmalm A. Acipimox stimulates skin blood flow by a cyclo-oxygenase-dependent mechanism. *Eur J Clin Pharmacol*. 1990;39(1):37–41.
30. Tunaru S, et al. PUMA-G and HM74 are receptors for nicotinic acid and mediate its anti-lipolytic effect. *Nat Med*. 2003;9(3):352–355.
31. Semple G, et al. 3-(1H-tetrazol-5-yl)-1,4,5,6-tetrahydro-cyclopentapyrazole (MK-0354): a partial agonist of the nicotinic acid receptor, G-protein coupled receptor 109a, with antilipolytic but no vasodilatory activity in mice. *J Med Chem*. 2008;51(16):5101–5108.
32. Walters RW, et al. beta-Arrestin1 mediates nicotinic acid-induced flushing, but not its antilipolytic effect, in mice. *J Clin Invest*. 2009;119(5):1312–1321.
33. Schaub A, Futterer A, Pfeffer K. PUMA-G, an IFN-gamma-inducible gene in macrophages is a novel member of the seven transmembrane spanning receptor superfamily. *Eur J Immunol*. 2001; 31(12):3714–3725.
34. Yousefi S, Cooper PR, Mueck B, Potter SL, Jarai G. cDNA representational difference analysis of human neutrophils stimulated by GM-CSF. *Biochem Biophys Res Commun*. 2000;277(2):401–409.
35. Thorburn J, Frankel AE, Thorburn A. Apoptosis by leukemia cell-targeted diphtheria toxin occurs via receptor-independent activation of Fas-associated death domain protein. *Clin Cancer Res*. 2003;9(2):861–865.
36. Morimoto H, Bonavida B. Diphtheria toxin- and Pseudomonas A toxin-mediated apoptosis. ADP ribosylation of elongation factor-2 is required for DNA fragmentation and cell lysis and synergy with tumor necrosis factor-alpha. *J Immunol*. 1992; 149(6):2089–2094.
37. Muller-Decker K, Scholz K, Neufang G, Marks F, Furstenberger G. Localization of prostaglandin-H synthase-1 and -2 in mouse skin: implications for cutaneous function. *Exp Cell Res*. 1998;242(1):84–91.
38. Wilgus TA, Ross MS, Parrett ML, Oberyszyn TM. Topical application of a selective cyclooxygenase inhibitor suppresses UVB mediated cutaneous inflammation. *Prostaglandins Other Lipid Mediat*. 2000;62(4):367–384.
39. Akunda JK, Lao HC, Lee CA, Sessoms AR, Slade RM, Langenbach R. Genetic deficiency or pharmacological inhibition of cyclooxygenase-1 or -2 induces mouse keratinocyte differentiation in vitro and in vivo. *FASEB J*. 2004;18(1):185–187.
40. Leong J, Hughes-Fulford M, Rakhlin N, Habib A, Maclouf J, Goldyne ME. Cyclooxygenases in human and mouse skin and cultured human keratinocytes: association of COX-2 expression with human keratinocyte differentiation. *Exp Cell Res*. 1996;224(1):79–87.
41. Pentland AP, Needleman P. Modulation of keratinocyte proliferation in vitro by endogenous prostaglandin synthesis. *J Clin Invest*. 1986;77(1):246–251.
42. Jonsson CE, Anggard E. Biosynthesis and metabolism of prostaglandin E 2 in human skin. *Scand J Clin Lab Invest*. 1972;29(3):289–296.
43. Williams TJ, Peck MJ. Role of prostaglandin-mediated vasodilatation in inflammation. *Nature*. 1977;270(5637):530–532.
44. Rosenbach T, Czernielewski J, Hecker M, Czarnetzki B. Comparison of eicosanoid generation by highly purified human Langerhans cells and keratinocytes. *J Invest Dermatol*. 1990;95(1):104–107.
45. Ujihara M, Horiguchi Y, Ikai K, Urade Y. Characterization and distribution of prostaglandin D synthetase in rat skin. *J Invest Dermatol*. 1988;90(4):448–451.
46. Dishy V, et al. Effects of aspirin when added to the prostaglandin D2 receptor antagonist laropiprant on niacin-induced flushing symptoms. *J Clin Pharmacol*. 2009;49(4):416–422.
47. Pedersen AK, FitzGerald GA. Dose-related kinetics of aspirin. Presystemic acetylation of platelet cyclooxygenase. *N Engl J Med*. 1984;311(19):1206–1211.
48. Cerletti C, et al. Pharmacokinetics of enteric-coated aspirin and inhibition of platelet thromboxane A2 and vascular prostacyclin generation in humans. *Clin Pharmacol Ther*. 1987;42(2):175–180.
49. Mitchell JA, Akarasereenont P, Thiemermann C, Flower RJ, Vane JR. Selectivity of nonsteroidal anti-inflammatory drugs as inhibitors of constitutive and inducible cyclooxygenase. *Proc Natl Acad Sci U S A*. 1993;90(24):11693–11697.
50. Nestle FO, Kaplan DH, Barker J. Psoriasis. *N Engl J Med*. 2009;361(5):496–509.
51. Wirth A, et al. G12-G13-LARG-mediated signaling in vascular smooth muscle is required for salt-induced hypertension. *Nat Med*. 2008;14(1):64–68.
52. Muyrers JP, Zhang Y, Testa G, Stewart AF. Rapid modification of bacterial artificial chromosomes by ET-recombination. *Nucleic Acids Res*. 1999; 27(6):1555–1557.
53. Moers A, et al. G13 is an essential mediator of platelet activation in hemostasis and thrombosis. *Nat Med*. 2003;9(11):1418–1422.
54. Lichti U, Anders J, Yuspa SH. Isolation and short-term culture of primary keratinocytes, hair follicle populations and dermal cells from newborn mice and keratinocytes from adult mice for in vitro analysis and for grafting to immunodeficient mice. *Nat Protoc*. 2008;3(5):799–810.
55. Baubet V, Le Mouellic H, Campbell AK, Lucas-Meunier E, Fossier P, Brulet P. Chimeric green fluorescent protein-aequorin as bioluminescent Ca2+ reporters at the single-cell level. *Proc Natl Acad Sci U S A*. 2000;97(13):7260–7265.